Velocity and Q in transverse isotropic media

Martin Karrenbach

ABSTRACT

Seismic velocity and Q measurements determine elastic and viscoelastic stiffness constants in a cross-well experiment. The methods described rely on picking direct wave traveltimes and determination of Q. Measured group velocity is converted to phase velocity, based on the assumption that wave propagation can be adequately described using plane waves. A general method is developed to invert for elastic and viscoelastic constants in a least-squares fit.

A practical determination scheme fits ellipses to dispersion relations of the medium. In a small angle approximation, elastic constants are deduced. This paraxial approximation is useful since it separates $v(z)$ effects from the intrinsic velocity anisotropy. Determined stiffness constants match model constants well where small angle measurements are used in a Greenhorn shale example.

INTRODUCTION

In the presence of transverse isotropy, the elastic constants of shale were determined in laboratory measurements and successfully recovered material constants (Tosaya, 1982, Podio et al., 1968, and Jones et al., 1981). All experiments were based on velocity measurements taken along the principal axes and at a 45° angle with respect to the symmetry plane. This experimental setting made it computationally easy to determine the elastic constants. In the laboratory, the rock specimen is readily accessible for measurement; the medium at the site is often only accessible in a limited way through wells and indirectly by surface experiments. Problems exist where one tries to extend laboratory measurements to *in situ* experiments.

A general problem is that all these experiments give a velocity; whether phase or group velocity is measured is difficult to say. Phase and group velocity can differ by as much as 8% for a Greenhorn shale example at different propagation angles. For the proposed inversion schemes, I assume group velocity is measured

and then convert it to phase velocity. I demonstrate a way to find elastic or viscoelastic constants in a transverse isotropic medium. A minimum of two wells is assumed in the area of interest. This general method has a pitfall: it leaves some stiffness constants more unconstrained than others, and, in the worst case, it leads to unrealistic values.

Using a determination scheme based on an elliptical approximation of disperion relations introduced by Muir and Dellinger (1985), I avoided this drawback. For small angles, I fitted elliptical curves to picked traveltime curves using least-squares. The Taylor expansion of the dispersion relation directly relates to the ellipse.

Using stiffness constants for Greenhorn shale (Jones et al., 1981), I found that determined elastic constants matched original constants well for small angle measurements. The small angle measurement ensures the distinction between $v(z)$ and *real* velocity anisotropy.

TRANSVERSE ISOTROPY

The stress/strain relationship in a general solid is given by

$$\sigma_{ij} = c_{ijkl}\,\epsilon_{kl} \qquad i,j,k,l = 1,2,3, \tag{1}$$

where $\sigma_{ij}, \epsilon_{kl}$ are the stress components and strain components, respectively, and c_{ijkl} are the elastic constants relating stress and strain.

In compressed notation, the transverse isotropic stiffness matrix takes on the form

$$\begin{pmatrix} \sigma_1 \\ \sigma_2 \\ \sigma_3 \\ \sigma_4 \\ \sigma_5 \\ \sigma_6 \end{pmatrix} = \begin{pmatrix} c_{11} & c_{12} & c_{13} & 0 & 0 & 0 \\ c_{12} & c_{11} & c_{13} & 0 & 0 & 0 \\ c_{13} & c_{13} & c_{33} & 0 & 0 & 0 \\ 0 & 0 & 0 & c_{44} & 0 & 0 \\ 0 & 0 & 0 & 0 & c_{44} & 0 \\ 0 & 0 & 0 & 0 & 0 & c_{66} \end{pmatrix} \begin{pmatrix} \epsilon_1 \\ \epsilon_2 \\ \epsilon_3 \\ \epsilon_4 \\ \epsilon_5 \\ \epsilon_6 \end{pmatrix}, \tag{2}$$

with $c_{66} = \frac{c_{11}-c_{12}}{2}$.

The equations of motion in terms of displacements (u, v, w) are:

$$\begin{aligned} c_{11}u_{xx} + c_{66}u_{yy} + c_{44}u_{zz} + (c_{12}+c_{66})v_{xy} + (c_{13}+c_{44})w_{xz} &= \rho u_{tt}, \\ c_{66}v_{xx} + c_{11}v_{yy} + c_{44}v_{zz} + (c_{12}+c_{66})u_{xy} + (c_{13}+c44)w_{xz} &= \rho v_{tt}, \end{aligned} \tag{3}$$

and

$$c_{44}w_{xx} + c_{44}w_{yy} + c_{33}w_{zz} + (c_{13}+c_{44})u_{xz} + (c_{13}+c_{44})v_{yz} = \rho w_{tt},$$

where the subscripts denote partial derivatives and ρ is the density. If we consider a plane wave propagating in x-z direction, particle displacement is given by

$$(u, v, w) = (b_1, b_2, b_3)e^{(x\cos\gamma + z\sin\gamma - vt)}. \tag{4}$$

V is the phase velocity of the plane wave and b_1, b_2 and b_3 are the displacement components. γ is the angle between the raypath and isotropic symmetry plane. Substituting this wave into the equations of motion (3) results in an algebraic system of equations:

$$\begin{aligned}(c_{11}\cos^2\gamma + c_{44}\sin^2\gamma)b_1 + (c_{13} + c_{44})\cos\gamma\sin\gamma &= \rho v^2 b_1\\ (c_{66}\cos^2\gamma + c_{44}\sin^2\gamma)\,b_2 &= \rho v^2 b_2\\ (c_{13} + c_{44})\cos\gamma\sin\gamma\, b_1 + (c_{44}\cos^2\gamma + c_{33}\sin^2\gamma)\,b_3 &= \rho v^2 b_3.\end{aligned} \tag{5}$$

Solving the system implies the determinant must vanish. These roots are the phase velocities of the plane waves in the given direction. In this way, we obtain three velocities:

$$\begin{aligned}v_1 = v_p &= \sqrt{\frac{c_{11}\cos^2\gamma + c_{33}\sin^2\gamma + c_{44} + \sqrt{D}}{2\rho}},\\ v_2 = v_{sv} &= \sqrt{\frac{c_{11}\cos^2\gamma + c_{33}\sin^2\gamma + c_{44} - \sqrt{D}}{2\rho}},\end{aligned} \tag{6}$$

and

$$v_3 = v_{sh} = \sqrt{\frac{c_{66}\cos^2\gamma + c_{44}\sin^2\gamma}{\rho}},$$

where $D = \{(c_{11} - c_{44})\cos^2\gamma - (c_{33} - c_{44})\sin^2\gamma\}^2 + 4(c_{13} + c_{44})^2\cos^2\gamma\sin^2\gamma$.

LABORATORY MEASUREMENTS

Tosaya (1982), Podio (1968) and Jones (1981) simplify the previous equations considerably by aligning the direction of propagation with the principal axes of the rock specimen. Letting the first subscript denote the direction of propagation and the second particle motion direction, we can easily measure the following quantities:

$$v_{11} = \sqrt{\frac{c_{11}}{\rho}}\ ,\ v_{12} = \sqrt{\frac{c_{66}}{\rho}}\ ,\ v_{13} = \sqrt{\frac{c_{44}}{\rho}} \tag{7}$$

along the x-direction

$$v_{33} = \sqrt{\frac{c_{33}}{\rho}}\ ,\ v_{31} = \sqrt{\frac{c_{44}}{\rho}}\ ,\ v_{32} = \sqrt{\frac{c_{44}}{\rho}} \tag{8}$$

along the z-direction. These velocities determine 4 out of 5 independent elastic constants. Just one more measurement, commonly chosen to be at an angle of 45° with respect to the symmetry plane is then needed, giving v_p^{45}. Measurements using rock samples are feasible, since all directions are readily accessible in the laboratory and small sample size guarantees that heterogeneities which could influence measurement accuracy are negligible.

Determination of the elastic constants from the above measurements is based upon the assumption that measured velocities are phase velocities. This might be true for raypaths along the principal axes; it is, however, not so for raypaths at the angles between these axes. Consequently, estimation of c_{13} is affected.

CONVERSION FROM GROUP TO PHASE VELOCITY

Velocity and direction of energy propagation are uniquely related to the velocity and direction of plane wave propagation in media with axisymmetric anisotropy. Dellinger and Muir (1985) give a detailed analysis of this transformation. Given group velocity U and energy propagation angle θ, phase velocity V is calculated by

$$V = \frac{U^2}{\sqrt{U^2 + (\frac{dU}{d\theta})^2}}, \tag{9}$$

and the angle of plane wave propagation γ by

$$\gamma = \theta - \arctan(\frac{(\frac{dU}{d\theta})}{U}). \tag{10}$$

Our measurements are always carried out in the group domain. I.e., we get the traveltime by determining the time at which a wave packet or energy blob arrives from a certain direction. Equations 5 and 6 are based on plane waves propagating through the medium. Consequently, measured group quantities have to be converted into plane wave quantities so as to utilize Equations 5 and 6. Transformations 9 and 10 can be carried out using finite differences. Alternatively, a small angle approximation can be used which carries out these transformations by fitting elliptical curves to the dispersion curves.

Greenhorn shale values are used to illustrate the discrepancy between group and phase velocity. Figure 1 shows group and phase velocity for the three different wave types in a polar plot. Distance from origin corresponds to magnitude of velocity given for this angular direction. In all plots velocities are normalized by horizontal phase velocity. Velocity values coincide when they meet at principal axes in all cases. In the off-axis region they differ in general. How large would the error in the velocity be if one measured group velocity in a certain direction and assumed that phase velocity was measured? See the velocity difference plot in Figure 1 for an answer. The sv-type wave shows the most anomalous behavior with a maximum 8 % difference between group and phase velocities at an angle of about 70°. The difference plot for this wave type shows only one-half the Hankel tail, which normally would be visible.

DETERMINATION OF ELASTIC CONSTANTS *IN-SITU*

The major problem in determining rock properties in the field is that measurement locations are heavily restricted to points at the surface and points in sparsely

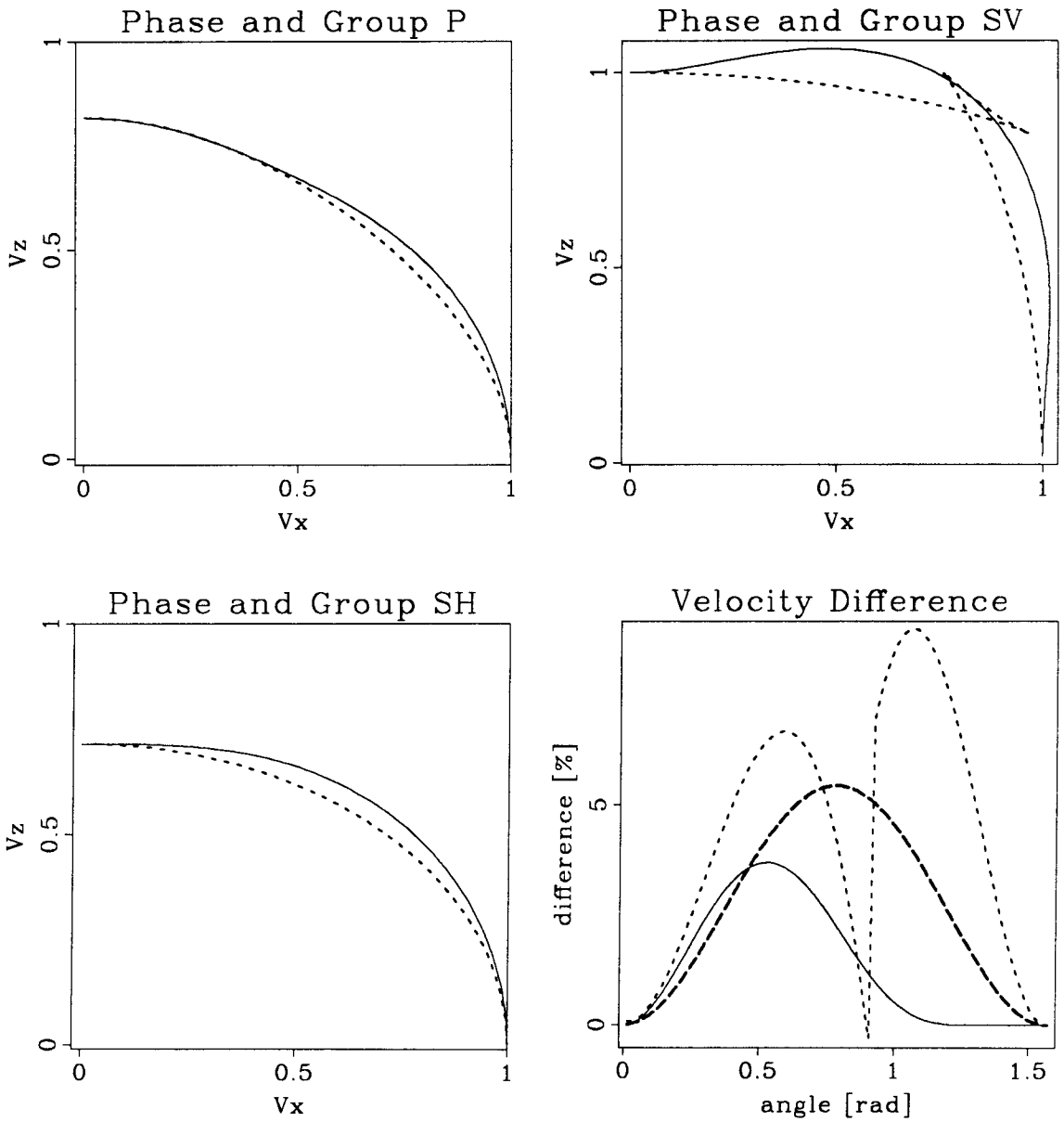

FIG. 1. Group (broken line) and phase (solid line) velocities for p-type, sv-type and sh-type waves in Greenhorn shale. Velocities are normalized to horizontal phase velocities. In the lower right panel the phase and group velocity differences for each wavetype are plotted against propagation angle: p = solid line, sv = thin broken line, sh = thick broken line.

available wells. Another difference between *in situ* and laboratory measurements is scale of experiment, which can differ in a few orders of magnitude. Extrapolation of laboratory data may cause problems and require *in situ* control. The necessity of taking *in situ* measurements is emphasized by the fact that the enviromental conditions of the rock are unchanged, whereas laboratory measurements can recreate the true environment only to a limited extent, if at all.

Where two wells exist in the area of investigation, an experiment configuration close to laboratory measurement conditions is available. Figure 2 shows v_{11}, v_{12} and v_{13} can be measured by placing sources and receivers at corresponding locations in the two wells. An ordinary pressure source whose signals are detected by a 3-component receiver can be used as a source. Non-linearity of the source interacting at the well interfaces will additionally generate shear waves. Signal-to-noise ratio in this case may not be high enough, especially if the rock material has a very low quality factor. Three component sources generating three different predominant wave types could be used to ensure clear signal detection.

Problems arise in determining velocities associated with propagation in the z-direction. In field experiments we are very unlikely to see a wave propagating at exactly 45° to the symmetry plane. *In situ* measurements in general are limited to raypath confined by a narrow fan. Fan width is then determined by the thickness of the rock under investigation since arrival times have to be picked on undisturbed direct waves. Figure 2 shows that fan width governs the maximum angle at which a wave will propagate with respect to the symmetry plane, implying measurements will have limited angular coverage and determination of elastic constants can be generalized to a least-squares problem.

From measurements we can determine the arrival time and distance travelled, if we assume straight raypaths. Amplitude of particle motion is given for picked arrival time. In equation (5) we can regard the elastic constants as unknown while particle motion $(b_{1_j}, b_{2_j}, b_{3_j})$, distance d_j, travel time t_j and angle γ_j are given by the jth measurement. We want to minimize the total error in the resulting system of equations:

$$E_1 = \sum_{j=1}^{n} [c_{11} \cos^2\gamma_j \, b_{1_j} - \rho(\frac{d_j}{t_j})^2 \, b_{1_j} + c_{13} \cos\gamma_j \sin\gamma_j \, b_{3_j} + c_{44} (\sin^2\gamma_j \, b_{1_j} + \cos\gamma_j \sin\gamma_j \, b_{3_j}]^2,$$

$$E_2 = \sum_{j=1}^{n} [c_{44} \sin^2\gamma_j \, b_{2_j} - \rho(\frac{d_j}{t_j})^2 \, b_{2_j} + c_{66} \cos^2\gamma_j \, b_{2_j} \,]^2, \qquad (11)$$

and

$$E_3 = \sum_{j=1}^{n} [-\rho(\frac{d_j}{t_j})^2 \, b_{3_j} + c_{13} \cos\gamma_j \sin\gamma_j \, b_{1_j} + c_{33} \sin^2\gamma_j \, b_{3_j} + c_{44} (\cos\gamma_j \sin\gamma_j \, b_{1_j} + (\cos^2\gamma_j \, b_{3_j}) \,]^2.$$

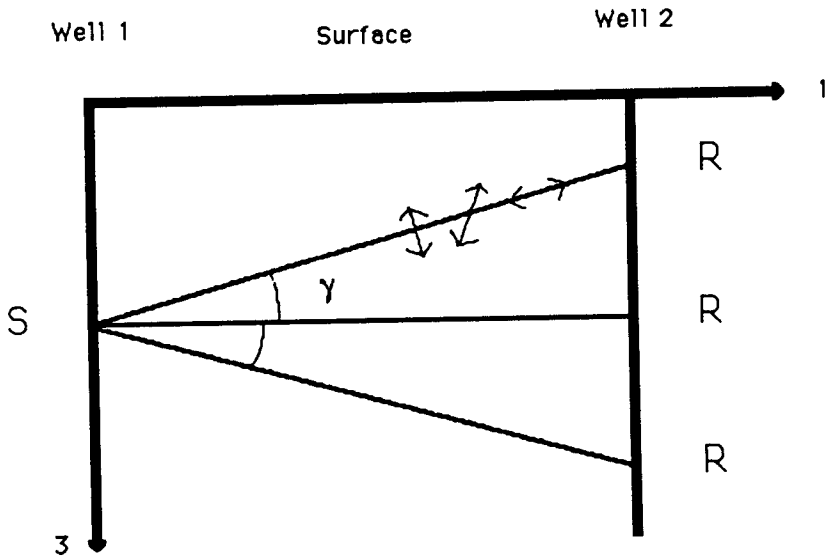

FIG. 2. Raypaths from source S to receiver R are at an angle γ to the horizontal bedding plane. Arrows indicate particle motion.

Consequently, we have to solve three systems of equations:

$$\sum_{j=1}^{n} \{F\ F^T\}\ X\ =\ Y$$

where F,X and Y are given by

$$F\ =\ \begin{pmatrix} -\rho\left(\frac{d_j}{t_j}\right)^2 b_{1_j} \\ \cos^2\gamma_j\ b_{1_j} \\ \cos\gamma_j\ \sin\gamma_j\ b_{3_j} \\ \sin^2\gamma_j\ b_{1_j}\ +\ \cos\gamma_j\ \sin\gamma_j\ b_{3_j} \end{pmatrix},\quad X\ =\ \begin{pmatrix} 1 \\ c_{11} \\ c_{13} \\ c_{44} \end{pmatrix},\quad Y\ =\ \begin{pmatrix} E_1 \\ 0 \\ 0 \\ 0 \end{pmatrix};$$

$$\sum_{j=1}^{n} \{GG^T\}\ X\ =\ Y$$

where G, X and Y are given by

$$G\ =\ \begin{pmatrix} -\rho\left(\frac{d_j}{t_j}\right)^2 b_{2_j} \\ \sin^2\gamma_j\ b_{2_j} \\ \cos^2\gamma_j\ b_{2_j} \end{pmatrix},\quad X\ =\ \begin{pmatrix} 1 \\ c_{44} \\ c_{66} \end{pmatrix},\quad Y\ =\ \begin{pmatrix} E_2 \\ 0 \\ 0 \end{pmatrix}; \tag{12}$$

and

$$\sum_{j=1}^{n} \{HH^T\}\ X\ =\ Y$$

where H, X and Y are given by

$$H = \begin{pmatrix} -\rho\left(\frac{d_j}{t_j}\right)^2 b_{3_j} \\ \cos\gamma_j \sin\gamma_j b_{1_j} \\ \sin^2\gamma_j b_{3_j} \\ \cos\gamma_j \sin\gamma_j b_{1_j} + \cos^2\gamma_j b_{3_j} \end{pmatrix}, \quad X = \begin{pmatrix} 1 \\ c_{13} \\ c_{33} \\ c_{44} \end{pmatrix}, \quad Y = \begin{pmatrix} E_3 \\ 0 \\ 0 \\ 0 \end{pmatrix},$$

where n is the total number of observations and ^{T} denotes the transpose. In this way we can determine the elastic constants in a least-squares sense. Values obtained can be cross-checked, since the constants c_{13} and c_{44} can be determined using independent measurements, due to the fact that these constants can be obtained using two different modes of propagation. If measurements and picks are consistent, values obtained from independent modes will coincide. The match indicates how trustworthy the observations are.

DETERMINATION OF VISCO-ELASTIC CONSTANTS *IN-SITU*

The method described above can easily be extended to determination of the viscoelastic constants, if not only traveltimes but also amplitude ratios are measured.

For these measurements, a configuration such as that in Figure 3 is favorable. Sources are placed in the first well and receivers in the second and third. Receivers in the second well record the wavelet as it traverses the well and represent a source wavelet estimate for the wave field recorded in the third well. Q measurements are commonly realized by comparing the power spectrum of the source wavelet with that of the power spectrum of the recorded wavelet. Traveltimes of the wave between the second and third well are measured in the usual way, replicating the above-mentioned configuration.

Take a plane wave as described in Equation 4, but allow the velocity to be complex. Thus, v is substituted by $v_{re} + i\, v_{im}$ and Equation 4 becomes

$$(u, v, w) = (b_1, b_2, b_3)\; e^{-v_{im}t}\; e^{(x\cos\gamma + z\sin\gamma - v_{re}t)}. \tag{13}$$

Since amplitude decays with distance travelled in the lossy material, we find the following definition for complex velocity appropriate:

$$v = v_{real} + i\, v_{real}\, Q^{-1}. \tag{14}$$

The real part is measured velocity v_{real}; the imaginary part is the product of the measured velocity times the reciprocal of quality factor Q. We can see that both velocity and Q have directional dependence. The least-squares normal equations for the elastic constants, Equation 12, consist of multiplication of a column vector by its transpose. This operation has to be changed: $\frac{d_j}{t_j}$ has to be replaced by $\frac{d_j}{t_j}(1 + iQ^{-1})$, and the complex conjugate transpose has to be multiplied, leaving us with the following system of equations to be solved:

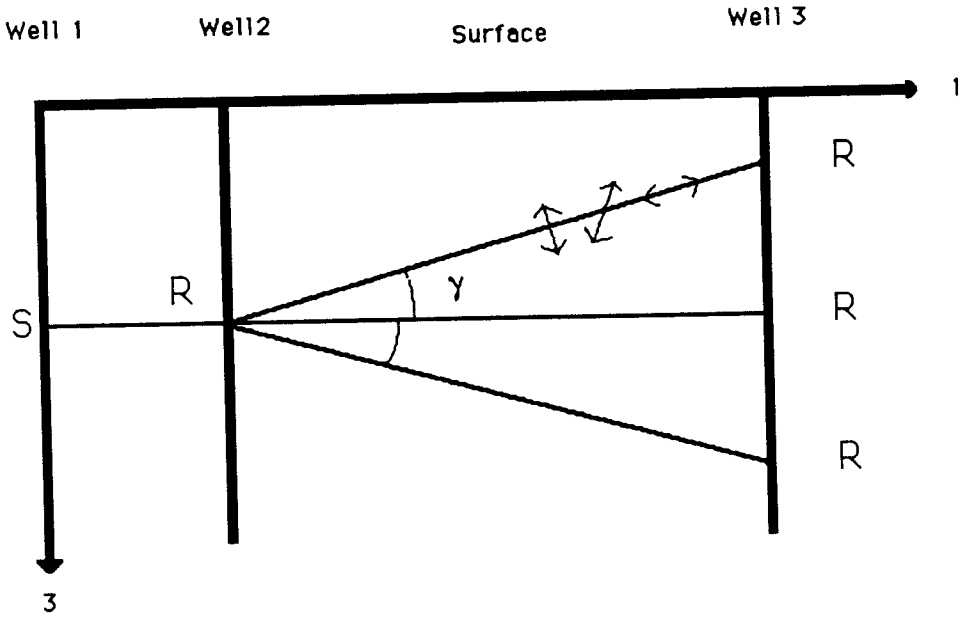

FIG. 3. A 3-well configuration is used to measure velocity and Q between Well 2 and Well 3. The signal recorded in Well 2 is a reference signal when compared with signals received in Well 3.

$$\sum_{j=1}^{n} \{FF^{*T}\}\, X = Y,$$

where F,X and Y are given by

$$F = \begin{pmatrix} -\rho\left(\frac{d_j}{t_j}\right)^2 \left[(1-Q^{-2}) + i2Q^{-1}\right] b_{1_j} \\ \cos^2\gamma_j\ b_{1_j} \\ \cos\gamma_j\ \sin\gamma_j\ b_{3_j} \\ \sin^2\gamma_j\ b_{1_j} + \cos\gamma_j\ \sin\gamma_j\ b_{3_j} \end{pmatrix}, \quad X = \begin{pmatrix} 1 \\ c_{11} \\ c_{13} \\ c_{44} \end{pmatrix}, \quad Y = \begin{pmatrix} E_1 \\ 0 \\ 0 \\ 0 \end{pmatrix};$$

$$\sum_{j=1}^{n} \{G\, G^{*T}\}\, X = Y$$

where G,X and Y are given by

$$G = \begin{pmatrix} -\rho\left(\frac{d_j}{t_j}\right)^2 \left[(1-Q^{-2}) + i2Q^{-1}\right] b_{2_j} \\ \sin^2\gamma_j\ b_{2_j} \\ \cos^2\gamma_j\ b_{2_j} \end{pmatrix}, \quad X = \begin{pmatrix} 1 \\ c_{44} \\ c_{66} \end{pmatrix}, \quad Y = \begin{pmatrix} E_2 \\ 0 \\ 0 \end{pmatrix}; \quad (15)$$

$$\sum_{j=1}^{n} \{H\ H^{*T}\}\ X\ =\ Y$$

where H,X and Y are given by

$$H\ =\ \begin{pmatrix} -\rho\left(\frac{d_j}{t_j}\right)^2\ [(1-Q^{-2})+i2Q^{-1}]\ b_{3_j} \\ \cos\gamma_j\ \sin\gamma_j\ b_{1_j} \\ \sin^2\gamma_j\ b_{3_j} \\ \cos\gamma_j\ \sin\gamma_j\ b_{1_j}\ +\ \cos^2\gamma_j\ b_{3_j} \end{pmatrix},\quad X\ =\ \begin{pmatrix} 1 \\ c_{13} \\ c_{33} \\ c_{44} \end{pmatrix},\quad Y\ =\ \begin{pmatrix} E_3 \\ 0 \\ 0 \\ 0 \end{pmatrix}.$$

Here ^{*T} denotes the complex conjugate transpose. The least-squares solutions for the viscoelastic constants will be complex numbers in contrast with the elastic case, where the constants were real numbers.

The assumption made here is that stress and strain are frequency dependent and show a phase lag with respect to each other. In the elastic case we assumed neither frequency dependence nor loss of energy due to viscous behavior exists, and consequently obtained the static elastic constants. Measuring Q, we approach the viscoelastic case, and realize that stress and strain are frequency dependent. The viscoelastic constants also show frequency dependence; we have to be aware of the fact that the results are only valid in the frequency limit imposed by the seismic wavelet.

A PRACTICAL DETERMINATION SCHEME

In practice, one tries to find elastic or viscoelastic constants in media which have a small vertical thickness compared with horizontal extension. If only ray-paths within the medium are used so as to avoid the influence of heterogeneities, observations will be limited by small angles, leading to problems in the least-squares inversion scheme. Some of the constants ($c_{11}, c_{44} and c_{66}$) are very well-constrained, while others like c_{13} and c_{33} are little constrained by the measurements and can assume physically meaningless values.

A practical procedure which circumnavigates these drawbacks is use of a paraxial approximation of the dispersion relations. This approximation fits elliptical curves as described by Muir and Dellinger (1985), and allows easy transform of group slowness curves into phase velocity curves.

Optimal constraint of the range of possible values for the elastic constants requires that we assume vertical checkshots were carried out from which the p wave arrival can be measured and from which c_{33} value can be deduced. The second assumption is that only measurements in a small angular range are available. Group slowness curve is approximated by the ellipse

$$M(\theta)\ =\ M_x\ \sin^2\theta\ +\ M_z\ \cos^2\theta, \tag{16}$$

where M_z is the vertical group slowness squared, M_x is the horizontal group slowness squared, and M is the resultant squared slowness for given angle θ.

For each of the three wave types, group slowness ellipses are fitted using least-squares. Resulting values for M_z and M_x are given by

$$M_z = \frac{\sum_{j=1}^{n}\left(\frac{\sin\theta_j}{u(\theta_j)}\right)^2 \sum_{j=1}^{n}\cos^4\theta_j - \sum_{j=1}^{n}\left(\frac{\cos\theta_j}{u(\theta_j)}\right)^2 \sum_{j=1}^{n}\sin^2\theta_j\cos^2\theta_j}{\sum_{j=1}^{n}\sin^4\theta_j \sum_{j=1}^{n}\cos^4\theta_j - \left(\sum_{j=1}^{n}\sin^2\theta_j\cos^2\theta_j\right)^2} \tag{17}$$

and

$$M_x = \frac{\sum_{j=1}^{n}\left(\frac{\cos\theta_j}{u(\theta_j)}\right)^2 \sum_{j=1}^{n}\sin^4\theta_j - \sum_{j=1}^{n}\left(\frac{\sin\theta_j}{u(\theta_j)}\right)^2 \sum_{j=1}^{n}\sin^2\theta_j\cos^2\theta_j}{\sum_{j=1}^{n}\sin^4\theta_j \sum_{j=1}^{n}\cos^4\theta_j - \left(\sum_{j=1}^{n}\sin^2\theta_j\cos^2\theta_j\right)^2}. \tag{18}$$

Using group-to-phase domain transformation we again obtain an elliptical curve for phase velocity v at any given angle γ:

$$v^2(\gamma) = \frac{1}{M_z}\sin^2\gamma + \frac{1}{M_x}\cos^2\gamma. \tag{19}$$

Direct determination of the elastic constants is now possible. If $^{(1)}$,$^{(2)}$ and $^{(3)}$ denote p-like, sv-like and sh-like wave types, respectively, we obtain:

$$c_{11} = \frac{\rho}{M_x^{(1)}},\ c_{44} = \frac{\rho}{M_x^{(2)}},\ c_{66} = \frac{\rho}{M_x^{(3)}}. \tag{20}$$

C_{13} value can be obtained by expanding the p-like dispersion relation for small angles and matching coefficients of powers in $\sin\gamma$:

$$c_{13} = -c_{44} + \sqrt{(\rho\Delta + c_{11} - c_{44})(c_{11} - c_{44})}. \tag{21}$$

(Δ is the difference $\frac{1}{M_z^{(1)}} - \frac{1}{M_x^{(1)}}$). It is also possible to get the value for c_{33} using the expansion of the sv-like dispersion relation, given here for completeness:

$$c_{33} = \rho\Delta + c_{44} + \frac{(c_{13} + c_{44})^2}{c_{11} - c_{44}}. \tag{22}$$

(Δ is the difference $\frac{1}{M_z^{(2)}} - \frac{1}{M_x^{(2)}}$ in this instance).

Notice the similarity to laboratory experiments here. What is different about this scheme is that it does take the difference between group and phase velocity into consideration, and uses raypaths which do not coincide with the principal axes of anisotropy, employing a paraxial approximation which makes perfectly sense for an *in situ* experiment. The procedure does not change for determination of viscoelastic constants.

Table 1 calculates elastic constants using the above scheme. Data points in regions with different angular coverage were used for fitting elliptical curves. Even for large angles c_{11}, c_{44} and c_{66} are recovered very well. For c_{13} and c_{33}, inverted values are increasingly different from correct values, indicating the discrepancy between actual dispersion relation and the elliptical curve.

Constants From Fitting Ellipses				
Constants [kbar]	Model	1° fit	10° fit	30° fit
c11	**341**	**341.02**	340.96	339.24
c44	**54**	**54.00**	54.04	54.20
c66	**106**	**106.00**	106.00	106.00
c13	**107**	**106.79**	109.98	123.86
c33	**227**	**226.64**	227.26	240.11

Table 1 Comparison between model and recovered stiffness constants using different maximum angular coverage.

CONCLUSIONS

Elastic and viscoelastic constants of rocks can be determined by seismic cross well measurements. The method described relies on picking traveltimes of direct waves and determining Q. Three component receivers are necessary to discriminate among various wave modes, and three component sources are desirable, but not required. Accuracy of results is mainly determined by the angular coverage of rays traversing the medium under investigation. It is assumed that wave propagation can be adequately described using plane waves. Measured group velocity is converted to phase velocity before stiffness constants are obtained by using least-squares. In the least-squares matrix, low angular coverage corresponds to poor conditioning of the matrix. Thus, for a reliable determination of stiffness constants it is best to use as many wave modes in as many directions as possible. A few stiffness constants can be obtained by using different modes independently and can then be used for cross-checking and estimating inversion reliability.

A practical determination method is given which consists of fitting elliptical curves to dispersion relations. This approximation is valid for small angles against the horizontal and allows a determination of stiffness constants strongly constrained in range of possible values.

REFERENCES

Dellinger, J. and Muir, F., 1985, Two domains of anisotropy, SEP-**44**, 59-62.

Muir, F. and Dellinger, J., 1985, A practical anisotropic system, SEP-**44**, 55-58.

Tosaya, C.A., 1982, Acoustical Properties of clay-bearing rocks, Ph.D. Thesis, Stanford University.

Jones, L.E.A., and Wang, H.F., 1981, Ultrasonic velocities in Creteaceous shales from the Williston Basin: Geophysics, **46**, 288-297.

Podio, A.L., Gregory, A.R., and Gray, K.E., 1968, Dynamic properties of dry and water-saturated Green River shale under stress: Soc. Petroleum Engr. Jour., **8**, 389-404.

斯坦福物探研究组

毕昂多 毕昂迪，乔恩 克莱尔伯特，史蒂文 科尔，卡洛斯 坎哈 菲尔霍，乔 德林杰，吉恩 克劳德 杜莱克，约翰 埃根，威廉 哈兰，乔 杰蒂卡，马丁 凯伦巴赫，克莱门特 卡斯特夫，弗郎西斯 米尔，大卫 尼科尔斯，理查德 奥特里尼，米哈依 波普维奇，乔斯 文 特理尔，玛它 伍德沃德，张林

第六十期

一九八九年五月

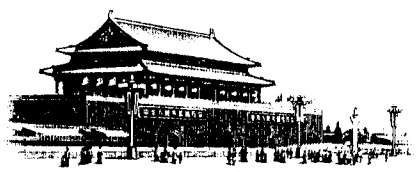

Chinese version of the cover page.